



Full Length Article

Experimental error assessment of laminar flame speed measurements for digital chemical kinetics databases

G. Walter^b, H. Wang^{a,*}, A. Kanz^b, A. Kolbasseff^c, X. Xu^d, O. Haidn^a, N. Slavinskaya^c^a Chair of Turbomachinery and Flight Propulsion, Technical University of Munich, 85748 Garching, Germany^b DLR German Aerospace Center, Institute of Combustion Technology, 70569 Stuttgart, Germany^c GRS Association for Plant and Reactor Safety, 85748 Garching, Germany^d School of Astronautics, Beihang University, 100191 Beijing, PR China

ARTICLE INFO

Keywords:

Laminar flame speed
Error assessment
Model optimization
Machine-readable files

ABSTRACT

This paper focuses on the uncertainty sources in experimental techniques applied for laminar flame speed measurements. The work was motivated due to the necessity to develop flexible standard sets of the key experimental parameters and descriptors to be included in the machine-readable files of digitalized data repositories such as ReSpeTh, PriMe, CloudFlame, etc. Besides identifying and making the data findable through the associated parameterized descriptions, available information should be interoperable with numerical codes evaluating uncertainty of experimental data. These uncertainty boundaries are very important for interpreters of the data and for development of statistical methods applied for the kinetic model optimization. On this way, four most common used techniques – Heat Flux Method (HFM), Bunsen Flame Method (BFM), Spherical Flame Method (SFM) and Counter Flow Method (CFM) were analyzed. The possible sources of experimental uncertainties have been investigated using data published by different research groups. Respective principles and structures of the experimental uncertainty sources for each studied method have been described. The uncertainty sources, their parameters and descriptors have been classified and systematically summarized in a universal data set to be used in the XML files of digitalized data repositories.

1. Introduction

Laminar flame speed (LFS) is one of the most important characteristics for combustion investigation. Accurate measurement and prediction of LFS is important for development and validation of kinetic models [1,2]. The main problem is that the different measuring methods exhibit large scatters for results. Moreover, even measurements performed with the same method but obtained employing different approaches and/or in different laboratories yield different results. In the past decades, great attention has been paid to the development of experimental techniques for measuring of LFS [3–10] and a number of excellent reviews on LFS measurements have been published over the years [10–14]. These reviews summarize remaining problems and challenges in the LFS measurements. The source of inaccuracy of LFS data, which unfortunately could not be avoided, follows from the equipment, experimental procedures, and data processing. Thus, one can classify two groups of uncertainty sources in flame speed measurements: equipment or “hardware” uncertainties and numerical interpretation of measured data, data processing (software)

uncertainties. The human factor might be assessed only by the experimentalists themselves.

To establish the numerical methods for objective evaluating the uncertainty of measured data, it is necessary to fix the different error sources and evaluate them quantitatively. That helps by expanding growth of the amount of experimental data to develop the advanced technologies for digitalized collecting data and making them findable, interoperable and interpretable (data mining). The machine-readable files should content all necessary information for that. In this paper we try to collect it for the LFS measurements. Therefore, our aim is not to establish an error assessment methodology for any particular measurement system, but to collect all basic uncertainty sources, their criteria and parameters and summarize them all together.

The past decades have seen a renewed improvement in uncertainty quantification and error assessment [15–18]. Gas phase reaction experimental database such as NIST Chemical Kinetic Database [19], ATcT database [20], ReSpecTh [21], CloudFlame [22,23] and PriMe [24] increased rapidly. PriMe [23–25] has received much attention as the prototype for ReSpecTh CloudFlame [22,23] and of the most

* Corresponding author.

E-mail address: hongxin.wang@tum.de (H. Wang).<https://doi.org/10.1016/j.fuel.2020.117012>

Received 21 June 2019; Received in revised form 16 December 2019; Accepted 2 January 2020

0016-2361/ © 2020 Elsevier Ltd. All rights reserved.

promising cyber systems offering kinetic database platforms, calculations and data analysis tools.

In the Warehouse, data is stored in form of Extensible Markup Language (XML) files. This format and its modifications are mostly used in digital databases and are easily compatible with numerical tools implemented for statistical data analysis [24–28]. The main fields, which should be included in such files for data submission, storage and analysis are analyzed and described in the presented paper concerning the four most common methods for LSF measurement – Heat Flux Method (HFM), Bunsen Flame Method (BFM), Spherical Flame Method (SFM) and Counter Flow Method (CFM).

The Section 2 shortly describes these experimental technologies for the determination of LFS. The sources of experimental uncertainty for each method are analyzed and summarized in the Section 3. The summary and conclusions are drawn in the final section. Open questions and future investigation are discussed in this section as well. We hope this work can promote and initiate the active discussion in kinetic community to find an optimal and objective form for presentation of the studied data in the digital form.

2. Experimental methods

In this part, an overview of four methods for LFS measurement is presented. Since a growing body of literature has examined the described experimental methods, only brief descriptions will be given here. However, as the numerical interpretation of measured data have less attention in then literature, we described those with same details. Details of designs of experimental installations are given in Supplement 1.

2.1. Bunsen flame method

Bunsen flame method is a traditional method used for laminar flame characteristic study [29–31]. A schematic of a Bunsen flame experiment system from He et al. [30] is shown in Fig. S1-1.

In this method, a conical flame under laminar flow condition is generated with a Bunsen burner. Once the conical flame has stabilized on the burner, it is then evaluated by optical methods such as streak photography or OH chemiluminescence [29]. A distinction can be made between two methods for determining the laminar flame velocity [30]. In the first case, it is assumed that the burning velocity is the same everywhere on the flame surface. The laminar flame velocity can then be calculated using the mass conservation rate:

$$\rho_u S_L A = \rho_u \dot{Q} \rightarrow S_L = \frac{\dot{Q}}{A},$$

where ρ_u is a density of unburned gas mixture; \dot{Q} –volume flow of the unburned gas mixture; S_L –laminar flame speed; A –a size of the flame surface.

In order to use this method, an area A is required. This area is determined by analyzing the recordings of the flame using various

programs (Fig. 1). In the Fig. 1, the Abel-inverted recording is illustrated. The Abel inversion is a reconstruction of a circular, axisymmetric and two-dimensional function based on their mapping. This sets 2-D limits of the flames based on the maximum OH emission.

In the second case, the angle of the conical flame is determined and used to calculate the flame velocity (Fig. 2). The determination of the angle is carried out as in the flame surface method by evaluating the recordings of the flame. This method is very convenient for straight-sided flames and requires aerodynamically contoured nozzles. Here, the speed of the gas mixture at the nozzle exit is assumed to be uniform and the laminar flame speed is then calculated:

$$\cos\left(\frac{\pi}{2} - \alpha\right) = \frac{S_L}{S_u} \rightarrow S_L = S_u \sin(\alpha)$$

2.2. Heat flux method

In 1993, de Goey and coworkers introduced the heat flux method for stabilizing adiabatic flat flames and measuring laminar flame speed [3]. Since then many studies on this method have been performed [32–34]. The principle of the heat flux method is to use the heat flow to determine the flame speed. Fig. 3 shows a schematic of a flat flame burner and its top view. The burner consists of a burner head, a burner plate and a plenum chamber [32]. The gas mixture absorbs heat from the burner plate, causing an increase of the local burning rate of the adiabatic flame as compared to the local burning rate of non-preheated gas mixture at the exit of the burner plate. That causes thereby a stabilizing of the flame: if the velocity of the unburned gas mixture, S_u , equal to the laminar flame velocity, S_L ($S_u = S_L$), then the stabilized state is reached. In this state, the heat loss of the flame q_f equals the heat gain of the gas mixture q_g ($q_f = q_g$), which causes the net heat flux $\Delta q_{(f-g)}$ is equal zero.

From this result the relation with the laminar flame speed can be deduced:

$$\lambda_f \frac{T_{ad} - T_{in}}{\delta_{rz}} = \dot{m} c_p (T_{in} - T_0) = \rho_u S_u c_p (T_{in} - T_0),$$

$$S_u = \lambda_f \frac{T_{ad} - T_{in}}{\delta_{rz} \rho_u c_p (T_{in} - T_0)} = S_L,$$

where δ_{rz} –width of the reaction zone; δ_{vz} –width of preheating zone; λ_f –thermal conductivity coefficient in the reaction zone; T_{ad} –adiabatic temperature of the flame; T_{in} –temperature at the boundary between the reaction and preheating zone; T_0 –initial temperature or surface temperature of the burner plate; \dot{m} –mass flow of the unburned gas mixture; ρ_u –density of unburned gas mixture; c_p –specific heat capacity of the gas mixture.

In order to stabilize an adiabatic flame, a heating jacket with hot water to heat up the unburnt gas flowing through the burner plate, which can compensate the heat loss of the flame [3]. Thermocouples are attached on the burner plate radially to measure the upstream

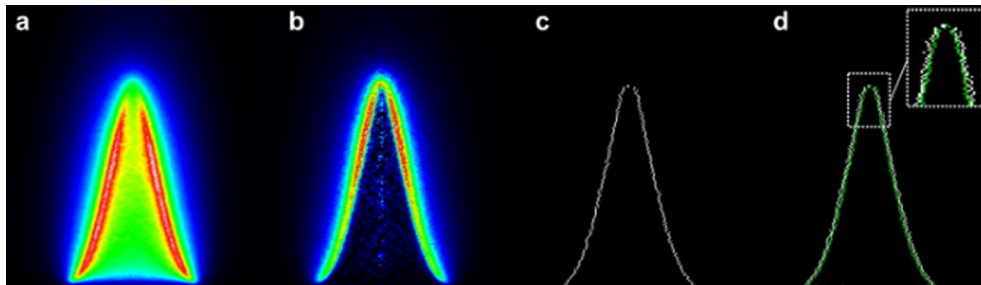


Fig. 1. Processing of OH chemiluminescence recording: (a) original recording; (b) Abel inverted image; (c) maximum intensified contour after Abel inversion; (d) superimposed outlines of the images with/without Abel inversion (). adopted from [30]

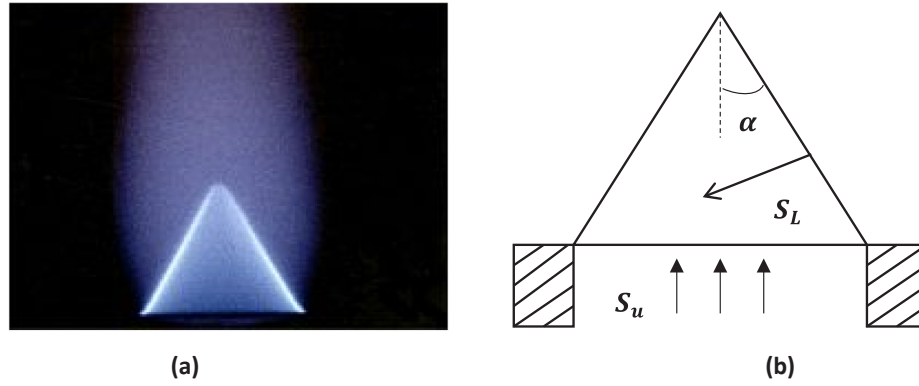


Fig. 2. Bunsen flame: (a) photograph of stoichiometric methane flame at 10 bar (DLR, Institute of Combustion Technology, Stuttgart); (b) schematic diagram of the conical Bunsen flame.

surface temperature of the burner plate, as shown in Fig. 3.

The objective here is to determine the inflow velocity at which the temperature profile over the entire surface of the burner plate is constant and corresponds to the temperature in the middle of the burner plate, where no heat losses occur. The measurements needed to determine are the temperature profile through the surface, $T_p(r)$, and velocity of unburned gas mixture, S_u . The measured temperature profile through the surface of the burner plate was analytically explained by de Goey et al. [3]. Later, Bosschaart and de Goey [34,35] simplified this temperature curve to the following equation:

$$T_p(r) = T_p(0) - \frac{\Delta q_{f-g}}{4\lambda_p b} r^2 \rightarrow T_p(r) = T_p(0) + \gamma r^2$$

where $\gamma = -\frac{\Delta q_{f-g}}{4\lambda_p b}$ is a parabolic coefficient and $T_p(r)$ —radial

temperature profile of the burner plate; $T_p(0)$ —temperature in the middle of the burner plate; b —width of the burner plate; λ_p —thermal conductivity of the burner plate in the radial direction; Δq_{f-g} —net heat flow. The adiabatic state is reached when the temperature profile is even or constant $T_p(r) = T_p(0)$. This is the case when $\gamma = 0$ and thus, $\Delta q_{f-g} = 0$, which describes the state where the heat losses in the burner plate are zero and can be neglected. The speed of the gas mixture S_u is varied and the respective radial temperature profiles are measured. Thereafter, the respective temperature profile is adjusted to the parabolic curve using the least squares method, with γ_i as the parabolic coefficient, Fig. 3b. The individual γ_i are adapted to a function $\gamma(S_u)$ using the method of least squares and then plotted as a function of corresponding incident velocities, Fig. 4.

It can be seen from the Fig. 4 that the velocity S_u equals $\gamma = 0$ (with $S_u = 35.4$ cm/s) and thus one also finds the laminar flame velocity S_L .

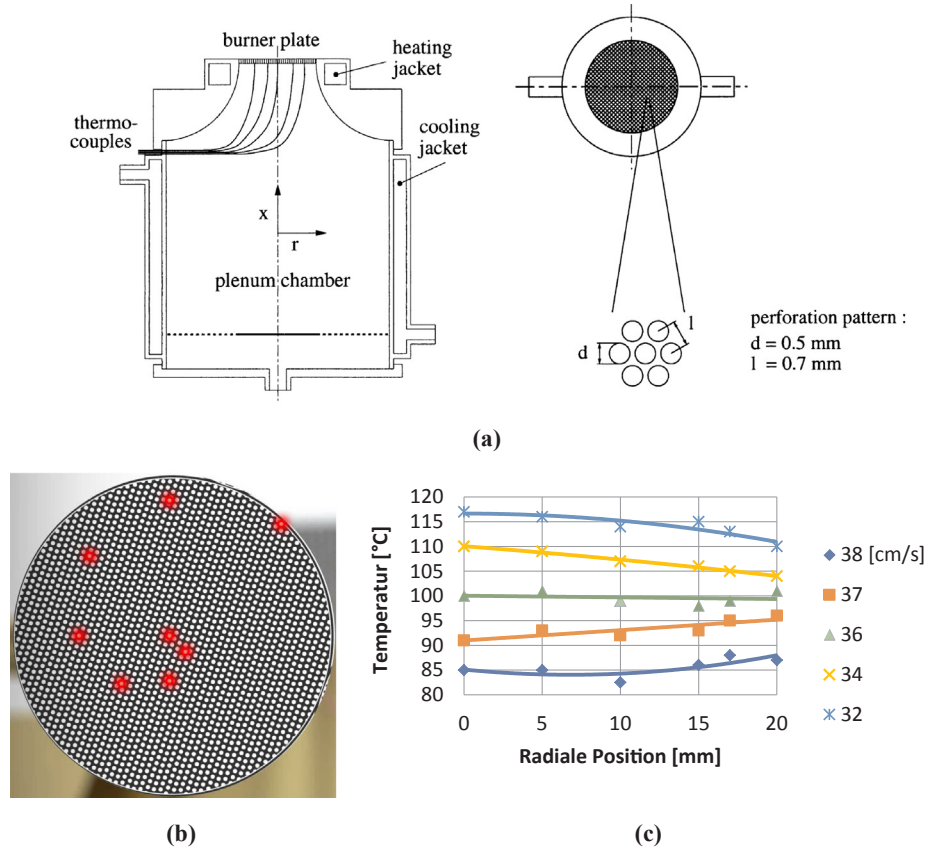


Fig. 3. (a) A schematic of a flat flame burner and its top view (b) Flat flame burner and the $T_p(r)$ measurements points; (c) typical $T_p(r)$ for different S_u .

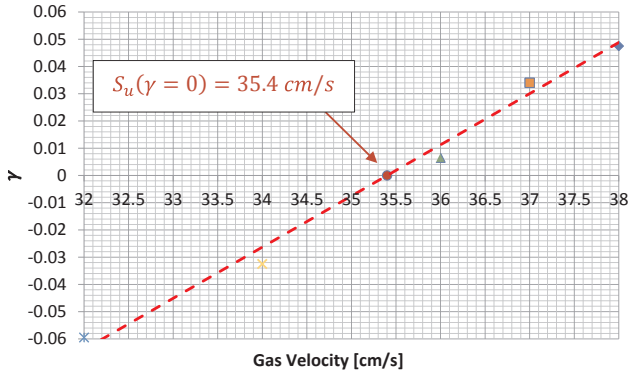


Fig. 4. An example of graphic for determining $\gamma = 0$ and thus $S_u = S_L$.

2.3. Spherical flame method

In the spherically symmetric flame, the radial propagation velocity of the spherically symmetric flame front is measured to derive the laminar flame velocity. Unlike other methods, which operational ranges are limited to a few atmospheres due to flame stability problems; this technic is applicable at elevated pressures and temperatures. Two methods can be used to measure flame speed in this methodology: recording the flame front-constant pressure method [36,37] and recording the pressure rise history constant volume [8,9,38] method.

In this method, the premixed fuel and air mixture are filled in the chamber with known initial temperature and pressure conditions. The mixture is centrally ignited and the propagation of the spherical flame front can be recorded with a high-speed camera, as shown in Fig. 5 [39]. Before the ignition, a vacuum state is established in the combustion chamber by a pumping system. The flame front to be examined is subject to a stretch or curvature. First, the radial propagation velocity of the flame, S_n , is calculated following $S_n = \frac{dr}{dt}$. The propagation velocity of the unstretched flame, S_b , is then obtained from Markstein length and stretch rate. After determining S_b , the laminar flame velocity, $S_{L,u}$, with respect to unburned mixture, is calculated from the

following continuity equation:

$$\rho_u S_{L,u} = \rho_b S_b \rightarrow S_{L,u} = S_b \frac{\rho_b}{\rho_u},$$

where ρ_b and ρ_u are the densities of the burned or unburned gas mixture.

2.4. Counterflow flame method

As described in [5,40–45], the basic principle of this method is to create a plane of stagnation by directing two identical gas mixture streams against each other. Ignition creates two flames, one on each side of the plane, as shown in Fig. 6. The objective here is to stabilize a flat as possible one-dimensional flame, which is necessary to investigate the structure, stability and extinction of pre-mixed and non-premixed flames [46–48].

The counterflow flames have a stretch effect, it makes the velocity vary with the nozzle radius [49,50]. The scale of stretch depends on the ratio of the nozzle distance to the nozzle diameter. Therefore, in this method, the axial velocities, $S_{u,ax}$, measured by Digital Particle Image Velocimetry (DPIV) technology as a function of the distance from the nozzle exit and the associated scale rates, K , are used to determine the laminar flame velocities, Fig. 7, [12,51]. The minimum of the measured axial velocity directly in front of the flame front is defined as the reference flame velocity, $S_{u,ref}$, and is plotted as a function of the associated scale rates defined as the slope. The ascertain data is then extrapolated either linearly or non-linearly to determine the strain-free reference flame velocity for $K = 0$, which is defined as the laminar flame velocity. The difference between linear and non-linear extrapolation is quite large, as the linear method tends to overestimate the laminar flame velocity.

3. Uncertainty sources analysis

How it was be already noted, the systematical uncertainty of LFS measurements follow from factors related to the experimental design (“hardware”) and procedure (“software”). In this part, the Section 3.1

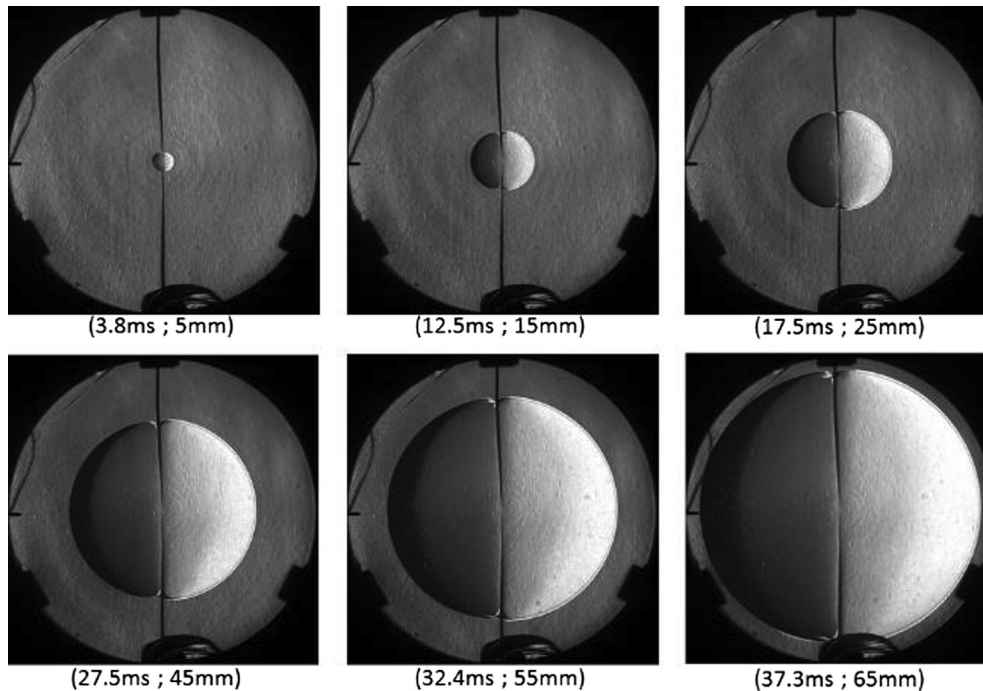
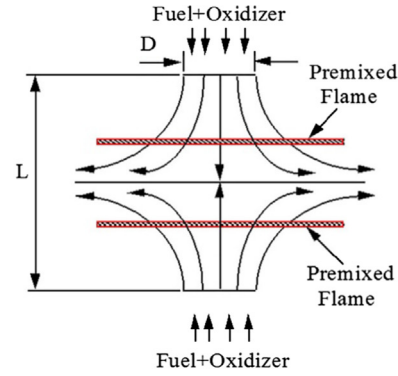


Fig. 5. Flame front propagation in the combustion chamber (). adopted from [39]



(a)



(b)

Fig. 6. Counterflow flame: a) image b) schematic [12].

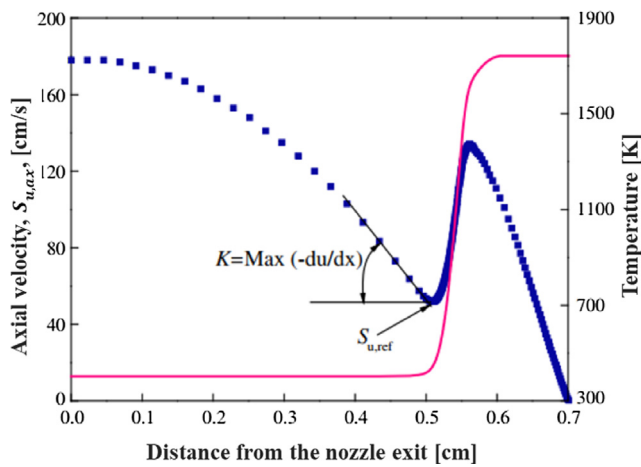


Fig. 7. Line: Temperature profile; Symbol: axial velocity profile (counterflow).
adopted from [6]

lists the uncertainty sources shared by four studied methods. Sections 3.2–3.5 analyzes the characteristics that are related to each individual analyzed method of the LFS determination.

3.1. Common uncertainty sources

Some systematical uncertainty sources related to manufacture, experimental condition deviations, measurement facilities, premixed mixture preparation, heat loss, etc. can be assumed as common for the studied methods. Unfortunately, we could not find the exact quantitative evaluations of these errors in the literature. The different estimations of individual factors were done in some studies [3,12,37,49,52–58]. The uncertainty boundaries for experimental devices are mostly given by manufacturers. The inaccuracy of thermocouple, pressure sensor and mass flow controller can be directly evaluated from recommendations of manufacturers. It is assumed that there is no independent (re)calibration. This characteristic can be replaced if a calibration is carried out. It is useful to note, that the calibration of the measuring instruments must be replicated with certain time intervals to obtain over time deviations.

The specific material properties of the burner may cause to inaccuracy in the LFS measuring [59,60] through unsmooth surface of the burner plate. It may have active sites with bound radicals, which can react with the fuel. These centers can also operate as catalysts, which can accelerate the reaction. This uncertainty source is considered to contribute 0.2% to the total uncertainty of LFS.

The uncertainty of the mixture preparation can follow from the composition of air, specific properties of the fuel and the premixed mixture stoichiometry [61,62]. There are three main sources of the air: compressed atmospheric air, factory made premixed O_2/N_2 gas in cylinders and O_2/N_2 mixture produced during the experiment. The inaccuracy of the dilution ratio is considered as 0.2%. The impurity in liquid fuel can result in inaccuracies of equivalence ratio. Some fuels leave vestiges in the evaporator or in the line, which may have unknown chemical reactions and change the composition of the fuel.

The chemical and physical properties of fuel influence the measurements uncertainties through possible reactions with devices and phase change. If the fuel is CO, the interaction of CO and the material of the gas cylinder wall can produce nickel carbonyl or iron carbonyl [63,64]. Considering that the flowing oscillation can lead to undesired changes in equivalence ratio and liquid fuels face a stronger oscillation than gaseous fuels due to the difference of supply system, there is a higher inaccuracy for liquid fuels than gaseous fuels, which are 0.5% and 0.2% for liquid and gaseous fuels respectively [61,62]. If the fuel is liquid, a heating tube will be used to prevent the condensation of the vaporized mixture on the way from the evaporator to the chamber, and a long heating tube will increase the error [32,65]. From the available database, it is deduced that the fluctuation of the flame velocities increases for quite lean and quite rich combustion, which can contribute 0.5% [5] to the uncertainty of LFS.

The experimental conditions, pressure and temperature are also sources for uncertainty of LFS determination [3,66–71]. The real pressure and temperature of the test may not be the desired ones. It has been observed that in high-pressure experiments, the flame becomes unstable at pressures higher than 4 atm due to the fact that the diffusion of the radicals is slowed down and thus the velocity decreases, so an uncertainty of 0.5% is added when the pressure is higher than 4 atm [5]. The influence of temperature can be evaluated following Alekseev et al. [11]:

$$S_{L,set} = S_{L,m} \left(\frac{T_{g,set}}{T_{g,set} + \Delta T_g} \right)^\alpha$$

where ΔT_g is the temperature deviation, $S_{L,set}$ is the LFS at the chosen temperature $T_{g,set}$, $S_{L,m}$ is the LFS at the measured temperature $T_{g,set} + \Delta T_g$, and α is the temperature exponent. The flame velocity $S_{L,set}$ is proportional to $(T_{g,set} + \Delta T_g)^{1-\alpha}$. Thus, applies to the error in the flame speed:

$$\frac{\Delta S_L}{S_L} = \frac{(1 - \alpha) \Delta T_g}{T_{g,set}}$$

For a small α , the inaccuracy of the LFS is negligibly small. However, for gas mixtures at the explosive limit, α is large enough and the inaccuracy of LFS can increase up to 2%.

Table 1
Common uncertainty sources for LFS measurement.

Source	Uncertainty (%)
Specific material properties of the burner	+0.2%
Mass flow controller	Λ^*
Pressure sensor	Λ^*
Thermocouple	Λ^*
Composition of the air	+0.2%
Specific properties of the fuel	Liquid: +0.5%
	Gaseous: +0.2%
Length of the heating tube	$L > 2 \text{ m}$: +0.2%
Stoichiometry	$\phi < 0.8$: +0.5%
	$\phi > 1.4$: +0.5%
Pressure	up to 1.5%
	$p > 4 \text{ atm}$: +0.5%
Temperature	Up to 2%
Radiation	Up to 2%
Numerical method	Basic: +0.05%
	Linear: +0.5%

* Λ is the measuring error self-calibrated or specified by the manufacturer.

The *heat loss* of the flame caused by radiation has an influence on the downstream temperature. According to study of Yu et al. [72], the radiation-induced uncertainty in the spherical flames is within 2%. Chen's work [73] indicated that the difference caused by radiation re-absorption is within 1%. So here we give a limitation of 2% for the uncertainty caused by radiation in the LFS measuring.

The *numerical interpretation of measured data* involves some inaccuracies that cannot be eliminated. For the extrapolation, a linear method of approximation tends to overestimate the laminar flame velocity, so an uncertainty of 0.5% is added when a linear method is used [32,74]. Moreover, every numerical method contribute 0.05% [58].

The common uncertainty sources for LFS measurement analyzed in this section are listed in Table 1. These uncertainty sources are very common in experimental works and are shared by the following four methods, so that they will not be discussed repeatedly. Except the measuring error determined by manufacturers, the errors of temperature and the heat loss caused by radiation contribute the two highest values to the total uncertainty. The error sources of properties of the reactants, the length of heating tube and numerical method can be reduced by making a better experiment design or choosing a good source of fuel and air. It is difficult to give exact quantitative evaluations of these errors, especially for some extreme conditions like high temperature and fuel lean cases. The values here, also in the following sections, are generally estimated based on the references and help with identification of different uncertainty sources.

3.2. Uncertainty sources for Bunsen flame method

The factors that influence the LFS determination in the Bunsen flame method are as follow:

- Nozzle geometry: A large nozzle contraction ratio is beneficial for keeping a steady laminar flow at the nozzle outlet [29].
- Length of the line burner: A ratio of line burner length and burner tube diameter higher than 50 can ensure a laminar flow [60].
- Diameter of the burner tube: A diameter of the burner tube between 4 mm and 12 mm is beneficial for the flame stability [29].
- Placement of the thermocouple: A thermocouple can be placed in the center of the burner to measure the temperature of the gas mixture. This thermocouple can interact with the laminar flow, which will lead to inaccuracy in the LFS [75].
- Height of the flame: A short flame will lead to an increase of the heat loss at the burner edge. On the contrary, a high flame will contribute to the expansion effect. Both of too short or too high flames can generate high uncertainty in the determination of LFS [76].

Table 2
Uncertainty sources for LFS measurement in Bunsen flame method.

Source	Uncertainty (%)
Nozzle geometry	+0.2%
Length of the line burner	$L/d < 50$: +0.2%
Diameter of the burner tube	$d > 12 \text{ mm}$: +0.5%
	$d < 4 \text{ mm}$: +0.5%
Placement of the thermocouple	Yes: +0.5%
Pilot flame	With pilot flame: +0.2%
	without pilot flame: +0.5%
Height of the flame	$h < 10 \text{ mm}$: +0.5%
	$h > 30 \text{ mm}$: +0.5%
H ₂ proportion (Syngas)	$[\text{H}_2] < 10\%$: +0.5%
	$[\text{H}_2] > 70\%$: +0.5%

- Pilot flame: Without a pilot flame, it is difficult to stabilize the jet flame because of the heat loss at the burner edge. However, the thermal effect of the pilot flame on the main flow cannot be neglected [76].
- H₂ proportion (Syngas): The LFS shows a linear development for H₂ content between 10% and 70%. Outside this range, the LFS shows an obvious non-linear variation and increasing fluctuation. In addition, a large H₂ proportion can lead to a rapid burning and make it difficult to stabilize the flame, and a low H₂ proportion with a higher CO fraction will cause poor burning [29].

Considering the above described factors, the uncertainty sources for LSF measurement in the Bunsen flame method are listed in Table 2.

3.3. Uncertainty sources for heat flux method

The factors that influence the LFS determination in the heat flux method are as follow:

- Diameter of the burner plate: Due to the interactions with ambient air, the edge effect can cause nonuniform distributions in the heat flux and radial diffusion. However, a quasi-one-dimensional laminar flame assumption can be applied to the central part of the flame surface. Its size is influenced by the stoichiometry, the speed of the gas mixture and the diameter of the burner plate. A burner plate with a larger diameter can lead to a larger central flame surface. On the contrary, a small burner plate diameter, especially in low-pressure conditions, makes the inaccuracy non-negligible because of the nonuniform effect on the laminar flame velocity [77,78].
- Cooling/Heating system: The temperature difference between the heated burner plate and the gas mixture has no direct influence on the flame speed, but affects the stabilization of the flame. A small temperature difference may cause a premature extinction to the flame. Therefore, it is important to keep the temperature difference large enough to ensure a stabilized laminar flame [11,79].
- Number of thermocouples: Blocking of the holes in the burner plate for thermocouples can affect the flame by interfering the uniformity of the gas mixture flow [12,32]. The error can be estimated by:

$$\text{error} = \frac{nA_{TE}}{A_{Br}},$$

with n —number of thermocouples; $A_{TE} = 4\pi r_{TE}^2$ —area of the holes, and $A_{Br} = 4\pi r_{Br}^2$ —surface of the burner.

Considering the above factors, the uncertainty sources for LSF measurement in the heat flux method are listed in Table 3.

3.4. Uncertainty sources for spherical flame method

The factors that influence the LFS determination in the spherical flame method are as follow:

Table 3
Uncertainty sources for LFS measurement in heat flux method.

Source	Uncertainty (%)
Diameter of the burner plate	$d < 16$ mm: +0.5%
Cooling/Heating system	$dT < 30$ K: +0.2%
Number of thermocouples	The percentage of blocked holes is then the gross error in LFS: e.g. 0.5% (of the 30 mm burner)

- (a) Product residues: Before each test, the chamber is rinsed several times with dry air to remove the residual products of the previous test, but it is possible that these products are not completely eliminated, which can affect the results of the new test [36,80].
- (b) Time to set a homogeneous condition: It takes time to reach the homogeneous state in the chamber, so that the condition may not be 100% homogeneous state when the mixture is ignited [7].
- (c) Ignition delay: The ignition delay can affect the recording time and make a source of error [81,82].
- (d) Measuring radius: For a small radius, the flame is influenced by the ignition and electrodes. For a large radius, the flame can be influenced by the wall effects (premature extinguishing of the flame, the assumption of constant pressure is no longer valid for the large radius) [58,83].
- (e) Thinning agent: The thermal-diffuse instability of the flame increases with increasing proportion of diluent, for example CO_2 diluent, since this reduces the H_2 content [38].
- (a) Considering the above factors, the uncertainty sources for LSF measurement in the spherical flame method are listed in Table 4.

3.5. Uncertainty sources for counterflow method

The factors that influence the LFS determination in the spherical flame method are as follow:

- (a) Nozzle geometry: The same as the Bunsen flame method, a large nozzle contraction ratio is beneficial for keeping a steady laminar flow at the nozzle outlet [45].
- (b) Nozzle distance-relationship: The ratio of nozzle pitch to nozzle diameter L/D has an influence on the rate of elongation and the one-dimensional flame assumption [43].
- (c) Silicone fluid particles: Silicone fluid articles can affect the composition of the fuel and its behavior [41,42,84].
- (d) Co-flow: A N_2 - CO flow can be used to shield the counterflow flame from the environment, otherwise the interaction between the flame and ambient air or radial diffusion can lead to the flame instability [41].

Considering the factors described above, the uncertainty sources for LSF measurement in the spherical flame method are listed in.

3.6. Optimization of XML-data

Based on the identified possible sources of uncertainty for the

Table 4
Uncertainty sources for LFS measurement in spherical flame method.

Source	Uncertainty (%)
Product residues	0.2%
Time to set a homogeneous Condition	0.5%
Ignition delay	0.5%
Measuring radius	$r < 7$ mm: 0.5%
	$r > \frac{r_{in,VK}}{2}$: 0.5%
	($r_{in,VK}$ is the inner radius of the combustion chamber)
Thinning agent	used: 0.5%

Table 5
Uncertainty sources for LFS measurement in counterflow flame method.

Source	Uncertainty (%)
Nozzle geometry	+0.2%
Nozzle distance-relationship	$L/D < 1$: +0.2%
	$L/D > 1$: +0.2%
Silicone fluid particles	+0.2%
Co-flow	Without co-flow: +0.5%

different methods for determining the laminar flame speed, the XML files, earlier used in PrIme, were extended with additive fields and indicators which describe the sources of the measured data uncertainty. Table 6 contains the information collected in the performed data error analysis. It is a universal list containing all possible uncertainty sources appearing in four studied laminar flame speed techniques of measurements described above. The methods are abbreviated as follows: heat flux method (HFM), Bunsen flame method (BF), spherical flame method (SF) and counterflow method (CF). The first column, Category, contains the categories of the error sources. The second column, Error Source, contains the error sources. The third column contents related methods. The column Property Name contains parameters that determine uncertainty sources. The last column Label contains the indicators of the error prescribed to parameters used in the developed XML file.

4. Summary and conclusion

Having analyzed a very large set of data [11,12,29,32,38,41–43,45,60,75–79,81–84]. We can conclude that researchers are reluctant to present detailed analyses of the uncertainty of their measured data. Very often, we have to follow from one reference to another one to find the background work, which describes the experimental facilities in detail and, probably, explains sources of possible errors. Very often, two publications are many years apart, so that the background work could be considered only approximatively.

Nevertheless, we analyzed experimental device configurations, diagnostics and experimental methodologies of the four techniques widely applied for the flame speed measurements and defined parameters and indicators, which describe the important sources of the experimental uncertainties. Some parameters are common for all four techniques and their minimal contribution to the error can be estimated to within 5%–6%, as shown in Table 1.

It is worth to note that the parameters which we describe are related to the systematical errors only and random errors have to be determined by investigators. Generally, parameters, which we collected in Tables 1–5, can be exactly determined only by each experimental group individually. How it follows from our evaluations, in ideal cases, systematic uncertainties, conditioned by peculiarities of each methodology, can reach 3%–4% for the Bunsen flame method, 1.5%–2% for the heat flux method, 3% for the spherical flame method and 1.5%–2% for the counterflow method.

The Table 6 presents the generalized factors, which we propose to include in the corresponding fields of XML files used for submission of experimental data in the digitalized data depositaries. Keywords, specifying the meaning of the properties, are machine and human interpretable and interoperable for further handle in numerical tools applied for uncertainty analysis.

Digitalized, parameterized descriptions of experimental devices and methodologies are today the fundamental processes of data storing and data mining. We would like to emphasize that this work is not a presentation of a final start-of-art in the LFS data uncertainty, but an invitation to discuss this problem with focus on the data structure for machine-readable files. One of the purposes of this work is to initiate the discussion devoted to the reporting studied experimental data. It is very useful and actual to establish the consortia of researchers for developing standards and rules for systematical cataloging data in a

Table 6
Summary of error parameters.

Category	Error Source	Method	Property Name	Label
Design	Burner plate diameter	HFM	BurnerDiameter	D
	Heating/Cooling System	HFM	BurnerHeadTemperature	T,B
			ChamberTemperature	T,C
	Number of thermocouples	HFM	BurnerDiameter	D
			PerforationDiameter	D,P
			NumberTC	N,TC
	Heating tube length	HFM, BF	TubeLength	L,T
	Burner tube length	BF	TubeLength	L,B
	Burner tube diameter	BF	BurnerTubeDiameter	D,B
	Thermocouple in the flow	BF	TCPresence	TC
	Pilot flame	BF	PilotFlame	PF
	Measuring radius	SF	RadiusMin	R,m
			RadiusChamber	R,ch
	Nozzle distance ratio	CF	NozzleDistance	L
			NozzleDiameter	D,N
Calibration	Co-Flow	CF	CoFlow	CF
	Calibrations	HFM, BF, SF, CF	OwnCalibration	OC
			ManufactureCalibrations	MC
	Mass flow controller	HFM, BF, SF, CF	MassFlowController	MFC
	Pressure controller	HFM, BF, SF, CF	PressureController	PC
	Coriolis mass flow controller	HFM, BF, SF, CF	CoriolisMassFlow Controller	CMFC
	Thermocouples	HFM, BF, SF, CF	TCScatter	TCS
			UnburntGasTemperature	T
	Temperature controller	BF, SF, CF	TemperatureController	TempC
	Fuel properties	HFM, BF, SF, CF	FuelProperties	F
Process	H ₂ -ratio (Syngas)	HFM, BF, SF, CF	H ₂ -ratio	H ₂ -R
	Pressure	HFM, BF, SF, CF	Pressure	P
	Equivalence ratio	HFM, BF, SF, CF	EquivalenceRatio	Phi
	Dilution	SF	Dilution	DL
			LinearExtrapolation	ExL
Linear or non-linear method		HFM, SF, CF	NonLinearExtrapolation	ExNL

machine-readable format and data exchange.

CRedit authorship contribution statement

G. Walter: Investigation, Software. **H. Wang:** Writing - original draft. **A. Kanz:** Writing - review & editing. **A. Kolbasseff:** Writing - original draft. **X. Xu:** Writing - review & editing. **O. Haidn:** Project administration, Funding acquisition. **N. Slavinskaya:** Conceptualization, Writing - review & editing.

Declaration of Competing Interest

The authors declare that they have no known competing financial interests or personal relationships that could have appeared to influence the work reported in this paper.

Acknowledgment

Authors would like to acknowledge the cooperation of domain experts within the combustion community that has been made possible through the SMARTCATS COST Action CM1303, *Chemistry of Smart Energies Carriers and Technologies*, coordinated by Dr. Mara de Joannon (Istituto di Ricerca sulla Combustione Consiglio Nazionale delle Ricerche, Napoli, Italia). In particular, the members of the working task group within the action for *Standard definition for data collection and mining toward a virtual chemistry of Smart Energy Carriers*, coordinated by Dr. Edward Blurock (Lund University, Sweden).

Appendix A. Supplementary data

Supplementary data to this article can be found online at <https://doi.org/10.1016/j.fuel.2020.117012>.

References

- [1] Park O, Veloo PS, Egolfopoulos FN. Flame studies of C2 hydrocarbons. *Proc Combust Inst* 2013;34(1):711–8.
- [2] Ravi S, Sikes TG, Morones A, Keese CL, Petersen EL. Comparative study on the laminar flame speed enhancement of methane with ethane and ethylene addition. *Proc Combust Inst* 2015;35(1):679–86.
- [3] de Goeij LPH, van Maaren A, Quax RM. Stabilization of adiabatic premixed laminar flames on a flat flame burner. *Combust Sci Technol* 1993;92(1–3):201–7.
- [4] Dong C, Zhou Q, Zhao Q, Zhang Y, Xu T, Hui S. Experimental study on the laminar flame speed of hydrogen/carbon monoxide/air mixtures. *Fuel* 2009;88(10):1858–63.
- [5] Ji C, Dames E, Wang YL, Wang H, Egolfopoulos FN. Propagation and extinction of premixed C5–C12 n-alkane flames. *Combust Flame* 2010;157(2):277–87.
- [6] Kumar S, Paul P, Mukunda H. Studies on a new high-intensity low-emission burner. *Proc Combust Inst* 2002;29(1):1131–7.
- [7] Xiouris C, Ye T, Jayachandran J, Egolfopoulos FN. Laminar flame speeds under engine-relevant conditions: uncertainty quantification and minimization in spherically expanding flame experiments. *Combust Flame* 2016;163:270–83.
- [8] Rallits C, Tremer G. Equations for the determination of burning velocity in a spherical constant volume vessel. *Combust Flame* 1963;7:51–61.
- [9] Babkin V, Kononenko YG. Equations for determining normal flame velocity in a constant-volume spherical bomb. *Combust Explos Shock Waves* 1967;3(2):168–71.
- [10] Rallits CJ, Garforth AM. The determination of laminar burning velocity. *Prog Energy Combust Sci* 1980;6(4):303–29.
- [11] Alekseev VA, Naucier JD, Christensen M, Nilsson EJK, Volkov EN, de Goeij LPH, et al. Experimental uncertainties of the heat flux method for measuring burning velocities. *Combust Sci Technol* 2015;188(6):853–94.
- [12] Egolfopoulos FN, Hansen N, Ju Y, Kohse-Höinghaus K, Law CK, Qi F. Advances and challenges in laminar flame experiments and implications for combustion chemistry. *Prog Energy Combust Sci* 2014;43:36–67.
- [13] Konnov AA, Mohammad A, Kishore VR, Kim NI, Prathap C, Kumar S. A comprehensive review of measurements and data analysis of laminar burning velocities for various fuel + air mixtures. *Prog Energy Combust Sci* 2018;68:197–267.
- [14] Ranzi E, Frassoldati A, Grana R, Cuoci A, Faravelli T, Kelley A, et al. Hierarchical and comparative kinetic modeling of laminar flame speeds of hydrocarbon and oxygenated fuels. *Prog Energy Combust Sci* 2012;38(4):468–501.
- [15] Russi T, Packard A, Feeley R, Frenklach M. Sensitivity analysis of uncertainty in model prediction. *J Phys Chem A* 2008;112(12):2579–88.
- [16] Tomlin AS. The use of global uncertainty methods for the evaluation of combustion mechanisms. *Reliab Eng Syst Saf* 2006;91(10–11):1219–31.
- [17] Tomlin AS. The role of sensitivity and uncertainty analysis in combustion modelling. *Proc Combust Inst* 2013;34(1):159–76.
- [18] Wang H, Sheen DA. Combustion kinetic model uncertainty quantification, propagation and minimization. *Prog Energy Combust Sci* 2015;47:1–31.
- [19] Mallard WG, Westley F, Herron J, Hampson RF, Frizzell D. NIST chemical kinetics

- database. Version 2Q98. Gaithersburg, MD: National Institute of Standards and Technology; 1998.
- [20] Ruscic B, Pinzon RE, Morton ML, von Laszewski G, Bittner SJ, Nijssure SG, et al. Introduction to active thermochemical tables: several “key” enthalpies of formation revisited. *J Phys Chem A* 2004;108(45):9979–97.
- [21] ReSpecTh, <http://respecth.chem.elte.hu>.
- [22] Goteng GL, Nettyam N, Sarathy SM. CloudFlame: cyberinfrastructure for combustion research. 2013 International Conference on Information Science and Cloud Computing Companion. IEEE; 2013. p. 294–9.
- [23] Reyno-Chiasson Z, Nettyam N, Goteng G, Speight M, Lee B, Baskaran S, et al. CloudFlame and PriMe: accelerating combustion research in the cloud. 9th International Conference on Chemical Kinetics. Ghent, Belgium. 2015.
- [24] Frenklach M. Transforming data into knowledge—process informatics for combustion chemistry. *Proc Combust Inst* 2007;31(1):125–40. <https://doi.org/10.1016/j.proci.2006.08.121>.
- [25] You X, Packard A, Frenklach M. Process informatics tools for predictive modeling: hydrogen combustion. *Int J Chem Kinet* 2012;44(2):101–16.
- [26] Feeley R, Seiler P, Packard A, Frenklach M. Consistency of a reaction dataset. *J. Phys. Chem. A* 2004;108(44):9573–83.
- [27] Frenklach M, Packard A, Seiler P, Feeley R. Collaborative data processing in developing predictive models of complex reaction systems. *Int J Chem Kinet* 2004;36(1):57–66.
- [28] Slavinskaya NA, Abbasi M, Starcke JH, Whitside R, Mirzayeva A, Riedel U, et al. Development of an uncertainty quantification predictive chemical reaction model for syngas combustion. *Energy Fuels* 2017;31(3):2274–97.
- [29] Bouvet N, Chauveau C, Gökalp I, Lee SY, Santoro RJ. Characterization of syngas laminar flames using the Bunsen burner configuration. *Int J Hydrogen Energy* 2011;36(1):992–1005.
- [30] He Y, Wang Z, Yang L, Whiddon R, Li Z, Zhou J, et al. Investigation of laminar flame speeds of typical syngas using laser based Bunsen method and kinetic simulation. *Fuel* 2012;95:206–13.
- [31] Zhen HS, Leung CW, Cheung CS, Huang ZH. Characterization of biogas-hydrogen premixed flames using Bunsen burner. *Int J Hydrogen Energy* 2014;39(25):13292–9.
- [32] Bosschaert K, de Goeij L. Detailed analysis of the heat flux method for measuring burning velocities. *Combust Flame* 2003;132(1–2):170–80.
- [33] Goswami M, van Griensven JGH, Bastiaans RJM, Konnov AA, de Goeij LPH. Experimental and modeling study of the effect of elevated pressure on lean high-hydrogen syngas flames. *Proc Combust Inst* 2015;35(1):655–62.
- [34] Bosschaert KJ, de Goeij LPH. The laminar burning velocity of flames propagating in mixtures of hydrocarbons and air measured with the heat flux method. *Combust Flame* 2004;136(3):261–9.
- [35] Bosschaert KJ. Analysis of the heat flux method for measuring burning velocities. CiteSeer 2002.
- [36] Dowdy DR, Smith DB, Taylor SC, Williams A. The use of expanding spherical flames to determine burning velocities and stretch effects in hydrogen/air mixtures. *Symp (Int) Combust* 1991;23:325–32. Elsevier.
- [37] Tse S, Zhu D, Law CK. Morphology and burning rates of expanding spherical flames in H_2/O_2 /inert mixtures up to 60 atmospheres. *Proc Combust Inst* 2000;28(2):1793–800.
- [38] Faghhi M, Chen Z. The constant-volume propagating spherical flame method for laminar flame speed measurement. *Sci. Bull.* 2016;61(16):1296–310.
- [39] Hartmann RM. Customized software and hardware applied to assessment of outwardly spherical flames using the pressure trace: a thermodynamic approach to improve accuracy of laminar flame speed measurements. *Int J Thermodyn* 2017;20(2):121–30.
- [40] Christensen M. Laminar burning velocity and development of a chemical kinetic model for small oxygenated fuels. Lund University; 2016.
- [41] Das AK, Kumar K, Sung C-J. Laminar flame speeds of moist syngas mixtures. *Combust Flame* 2011;158(2):345–53.
- [42] Kumar K, Sung C-J, Hui X. Laminar flame speeds and extinction limits of conventional and alternative jet fuels. *Fuel* 2011;90(3):1004–11.
- [43] Vagelopoulos C, Egoopoulos FN, Law CK. Further considerations on the determination of laminar flame speeds with the counterflow twin-flame technique. *Sym (Int) Combust* 1994;25:1341–7. Elsevier.
- [44] Vagelopoulos CM, Egoopoulos FN. Direct experimental determination of laminar flame speeds. *Symp (Int) Combust* 1998;27(1):513–9.
- [45] Chao B, Egoopoulos F, Law CK. Structure and propagation of premixed flame in nozzle-generated counterflow. *Combust Flame* 1997;109(4):620–38.
- [46] Tsuji H, Yamaoka I. Structure and extinction of near-limit flames in a stagnation flow. *Symp (Int) Combust* 1982;19(1):1533–40. [https://doi.org/10.1016/S0082-0784\(82\)80330-5](https://doi.org/10.1016/S0082-0784(82)80330-5).
- [47] Seiser R, Pitsch H, Seshadri K, Pitz W, Gurran H. Extinction and autoignition of n-heptane in counterflow configuration. *Proc Combust Inst* 2000;28(2):2029–37.
- [48] Ahmed S, Balachandran R, Mastorakos E. Measurements of ignition probability in turbulent non-premixed counterflow flames. *Proc Combust Inst* 2007;31(1):1507–13.
- [49] Law CK. Dynamics of stretched flames. *Symp (Int) Combust* 1989;22:1381–402. Elsevier.
- [50] Matalon M. On flame stretch. *Combust Sci Technol* 1983;31(3–4):169–81.
- [51] Kee RJ, Miller JA, Evans GH, Dixon-Lewis G. A computational model of the structure and extinction of strained, opposed flow, premixed methane-air flames. *Symp (Int) Combust* 1989;22:1479–94. Elsevier.
- [52] Wu CK, Law CK. On the determination of laminar flame speeds from stretched flames. *Symp (Int) Combust* 1985;20(1):1941–9. [https://doi.org/10.1016/S0082-0784\(85\)80693-7](https://doi.org/10.1016/S0082-0784(85)80693-7).
- [53] Qin X, Ju Y. Measurements of burning velocities of dimethyl ether and air premixed flames at elevated pressures. *Proc Combust Inst* 2005;30(1):233–40.
- [54] Chen Z, Qin X, Ju Y, Zhao Z, Chaos M, Dryer FL. High temperature ignition and combustion enhancement by dimethyl ether addition to methane–air mixtures. *Proc Combust Inst* 2007;31(1):1215–22.
- [55] Varea E, Modica V, Vandel A, Renou B. Measurement of laminar burning velocity and Markstein length relative to fresh gases using a new postprocessing procedure: application to laminar spherical flames for methane, ethanol and isooctane/air mixtures. *Combust Flame* 2012;159(2):577–90.
- [56] Tahtouh T, Halter F, Mounaïm-Rousselle C. Measurement of laminar burning speeds and Markstein lengths using a novel methodology. *Combust Flame* 2009;156(9):1735–43.
- [57] Huo J, Yang S, Ren Z, Zhu D, Law CK. Uncertainty reduction in laminar flame speed extrapolation for expanding spherical flames. *Combust Flame* 2018;189:155–62.
- [58] Sikes T, Mannan MS, Petersen EL. An experimental study: laminar flame speed sensitivity from spherical flames in stoichiometric CH_4 –air mixtures. *Combust Sci Technol* 2018;190(9):1594–613.
- [59] Andrews G, Bradley D. Determination of burning velocities: a critical review. *Combust Flame* 1972;18(1):133–53.
- [60] Wang Z, Weng W, He Y, Li Z, Cen K. Effect of H_2/CO ratio and N_2/CO_2 dilution rate on laminar burning velocity of syngas investigated by direct measurement and simulation. *Fuel* 2015;141:285–92.
- [61] Santner J, Haas FM, Dryer FL, Ju Y. High temperature oxidation of formaldehyde and formyl radical: a study of 1, 3, 5-trioxane laminar burning velocities. *Proc Combust Inst* 2015;35(1):687–94.
- [62] Chen Z. On the accuracy of laminar flame speeds measured from outwardly propagating spherical flames: methane/air at normal temperature and pressure. *Combust Flame* 2015;162(6):2442–53.
- [63] Wang Z. Measurement of laminar burning speed and flame instability study of syngas/oxygen/helium premixed flame. Northeastern University; 2016.
- [64] Li H-M, Li G-X, Sun Z-Y, Zhai Y, Zhou Z-H. Measurement of the laminar burning velocities and markstein lengths of lean and stoichiometric syngas premixed flames under various hydrogen fractions. *Int J Hydrogen Energy* 2014;39(30):17371–80.
- [65] Dyakov IV, Konnov AA, Ruyck JD, Bosschaert KJ, Brock ECM, de Goeij LPH. Measurement of adiabatic burning velocity in methane-oxygen-nitrogen mixtures. *Combust Sci Technol* 2001;172(1):81–96.
- [66] Halter F, Chauveau C, Djebaili-Chaumeix N, Gökalp I. Characterization of the effects of pressure and hydrogen concentration on laminar burning velocities of methane–hydrogen–air mixtures. *Proc Combust Inst* 2005;30(1):201–8.
- [67] Rozenchan G, Zhu D, Law CK, Tse S. Outward propagation, burning velocities, and chemical effects of methane flames up to 60 atm. *Proc Combust Inst* 2002;29(2):1461–70.
- [68] Hassan MI, Aung KT, Faeth GM. Measured and predicted properties of laminar premixed methane/air flames at various pressures. *Combust Flame* 1998;115(4):539–50.
- [69] Egoopoulos FN, Cho P, Law CK. Laminar flame speeds of methane-air mixtures under reduced and elevated pressures. *Combust Flame* 1989;76(3–4):375–91.
- [70] Kurata O, Takahashi S, Uchiyama Y. Influence of preheat temperature on the laminar burning velocity of methane-air mixtures. *SAE Trans* 1994;1766–72.
- [71] Ogami Y, Kobayashi H. Laminar burning velocity of stoichiometric CH_4 /air premixed flames at high-pressure and high-temperature. *JSME Int J Ser B* 2005;48(3):603–9.
- [72] Yu H, Han W, Santner J, Gou X, Sohn CH, Ju Y, et al. Radiation-induced uncertainty in laminar flame speed measured from propagating spherical flames. *Combust Flame* 2014;161(11):2815–24.
- [73] Chen Z. Effects of radiation and compression on propagating spherical flames of methane/air mixtures near the lean flammability limit. *Combust Flame* 2010;157(12):2267–76.
- [74] Hu E, Chen Y, Zhang Z, Li X, Cheng Y, Huang Z. Experimental study on ethane ignition delay times and evaluation of chemical kinetic models. *Energy Fuels* 2015;29(7):4557–66.
- [75] Yilmaz N, Gill W, Donaldson AB, Lucero R. Problems encountered in fluctuating flame temperature measurements by thermocouple. *Sensors* 2008;8(12):7882–93.
- [76] Natarajan J, Kochar Y, Lieuwen T, Seitzman J. Laminar flame speeds of H_2 , CO , O_2 , he mixtures at elevated pressure and preheat temperature. Charlottesville, VA: Technical Meeting Eastern States Section of the Combustion Institute, University of Virginia; 2007. p. 1–9.
- [77] Konnov AA, Riemeijer R, de Goeij L. Adiabatic laminar burning velocities of $CH_4 + H_2 +$ air flames at low pressures. *Fuel* 2010;89(7):1392–6.
- [78] Konnov AA, Riemeijer R, Kornilov V, de Goeij L. 2D effects in laminar premixed flames stabilized on a flat flame burner. *Exp Therm Fluid Sci* 2013;47:213–23.
- [79] Yu J, Yu R, Fan X, Christensen M, Konnov A, Bai X-S. Onset of cellular flame instability in adiabatic $CH_4/O_2/CO_2$ and CH_4 /air laminar premixed flames stabilized on a flat-flame burner. *Combust Flame* 2013;160(7):1276–86.
- [80] Champion M, Deshaies B, Joulin G, Kinoshita K. Spherical flame initiation: theory versus experiments for lean propane air mixtures. *Combust Flame* 1986;65(3):319–37.
- [81] Troshin KY, Borisov A, Rakhmetov A, Arutyunov V, Politenkova G. Burning velocity of methane-hydrogen mixtures at elevated pressures and temperatures. *Russ J Phys Chem B* 2013;7(3):290–301.
- [82] Wu Y. Experimental investigation of laminar flame speeds of kerosene fuel and second generation biofuels in elevated conditions of pressure and preheat temperature. INSA: Rouen; 2016.
- [83] Taylor SC. Burning velocity and the influence of flame stretch. University of Leeds; 1991.
- [84] Huang Y, Sung C, Eng J. Laminar flame speeds of primary reference fuels and reformer gas mixtures. *Combust Flame* 2004;139(3):239–51.